Molecular Biophysics:

Reconstitution of Actin-based Motility by Vasodilator-stimulated Phosphoprotein (VASP) Depends on the Recruitment of F-actin Seeds from the Solution Produced by Cofilin

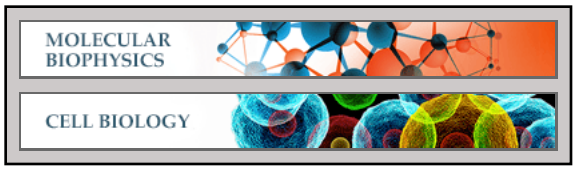

Orit Siton and Anne Bernheim-Groswasser

J. Biol. Chem. 2014, 289:31274-31286.
doi: 10.1074/jbc.M114.586958 originally published online September 22, 2014

THE JOURNAL OF BIOLOGICAL CHEMISTRY VOL. 289, NO. 45, pp. 31274–31286, November 7, 2014

Reconstitution of Actin-based Motility by Vasodilator-stimulated Phosphoprotein (VASP) Depends on the Recruitment of F-actin Seeds from the Solution Produced by Cofilin*[S]

Received for publication, June 5, 2014, and in revised form, September 6, 2014 Published, JBC Papers in Press, September 22, 2014, DOI 10.1074/jbc.M114.586958

Orit Siton and Anne Bernheim-Groswasser[1]

From the Department of Chemical Engineering and the Ilse Katz Institute for Nanoscale Science and Technology, Ben-Gurion University of the Negev, Beer-Sheva 84105, Israel

Background: Ena/VASP proteins play major roles in cell and pathogen motility.
Results: VASP promotes motility by recruiting F-actin seeds produced by cofilin, while competing with CPs with efficiency that depends on profilin concentration.
Conclusion: Recruitment of F-actin seeds is necessary for bundle formation and motility by VASP.
Significance: Freshly polymerized actin produced by cofilin at the leading edge is important for VASP function in cells.

Vasodilator-stimulated phosphoprotein (VASP) is active in many filopodium-based and cytoskeleton reorganization processes. It is not fully understood how VASP directly functions in actin-based motility and how regulatory proteins affect its function. Here, we combine bead motility assay and single filament experiments. In the presence of a bundling component, actin bundles that grow from the surface of WT-VASP-coated beads induced movement of the beads. VASP promotes actin-based movement alone, in the absence of other actin nucleators. We propose that at physiological salt conditions VASP nucleation activity is too weak to promote motility and bundle formation. Rather, VASP recruits F-actin seeds from the solution and promotes their elongation. Cofilin has a crucial role in the nucleation of these F-actin seeds, notably under conditions of unfavorable spontaneous actin nucleation. We explored the role of multiple VASP variants. We found that the VASP-F-actin binding domain is required for the recruitment of F-actin seeds from the solution. We also found that the interaction of profilin-actin complexes with the VASP-proline-rich domain and the binding of the VASP-F-actin binding domain to the side of growing filaments is critical for transforming actin polymerization into motion. At the single filament level, profilin mediates both filament elongation rate and VASP anti-capping activity. Binding of profilin-actin complexes increases the polymerization efficiency by VASP but decreases its efficiency as an anti-capper; binding of free profilin creates the opposite effect. Finally, we found that an additional component such as methylcellulose or fascin is required for actin bundle formation and motility mediated by VASP.

Ena/VASP[2] proteins play important roles in many cellular processes, including actin-based movement of cells and the bacterial pathogen *Listeria monocytogenes* (1–3), fibroblast migration (4), filopodia formation (5, 6) (in conjunction with the actin-bundling protein fascin), axon growth and guidance (7–9), and cell shape and morphology changes (10). Ena/VASP contains an N-terminal EVH1, a proline-rich domain, and a C-terminal EVH2 domain. The EVH1 domain is required for recruiting Ena/VASP proteins to their sites of action. The proline-rich domain binds profilin or profilin-actin complexes. The EVH2 domain binds actin monomers (actin) and filaments (F-actin) via its GAB- and FAB-binding sites, respectively, and terminates with a coiled-coil region that mediates Ena/VASP tetramerization. Because the major pool of actin polymerization components is profilin-actin complexes (11), filament elongation by VASP depends on its ability to recruit and incorporate the complexes onto the filament barbed end (12–14).

Numerous *in vivo* and *in vitro* studies were conducted to uncover the role of Ena/VASP proteins in actin-based processes, notably actin-based motility. Contradictory results were obtained both *in vivo* (4) and *in vitro* (15–20). The main objective of previous *in vitro* studies was to investigate how VASP mediates Arp2/3 complex-dependent actin polymerization (2, 15–18), yet none of these assays investigated how VASP functions alone in actin-based motility. Moreover, how actin polymerization mediated by VASP is translated into directed motion and the role of the actin regulatory proteins, profilin, capping proteins (CPs), and cofilin in these processes were not investigated. The effect of profilin on filament elongation by VASP was shown previously, yet contradictory results were observed (12, 21–23). VASP anti-capping (AC) activity is associated with the ability of VASP to compete with CPs for barbed end attachment and delay capping (12, 21, 22, 24). Profilin was suggested to have a positive effect on VASP AC activity (21, 22),

* This work was supported by Israel Science Foundation Grant 1534/10 (to A. B.-G.)
[S] This article contains supplemental Movies 1–10.
[1] To whom correspondence may be addressed: Dept. of Chemical Engineering, Ben-Gurion University of the Negev, Beer-Sheva 84105, Israel. Tel.: 972-8-647-2149; Fax: 972-8-646-2916; E-mail: bernheim@bgu.ac.il.
[2] The abbreviations used are: Ena/VASP, enabled/vasodilator-stimulated phosphoprotein; AC, anti-capping; F-actin, actin filament; CP, capping protein; FAB, F-actin binding domain; FRAP, fluorescent recovery after photobleaching; TIRF, total internal reflection fluorescence; NEM, *N*-ethylmaleimide; MC, methylcellulose; cryo-TEM, cryo-transmission electron microscopy; TIRFM, total internal reflection fluorescence microscopy; tβ4, thymosin-β4.

although the dependence of VASP AC activity on profilin concentration was measured in pyrene assays (21) and not directly at the individual filament level. Finally, the effect of cofilin on VASP function was not addressed in the past, despite the fact that both proteins are implicated in the formation and turnover of actin networks in cells (4, 10, 25–28). Although VASP and cofilin have been shown to be implicated in neuronal outgrowth and guidance (7, 29–36), the impact of cofilin on VASP activity has never been studied explicitly *in vivo* or *in vitro*.

By combining single filament experiment and bead motility assay, we show that VASP promotes actin-based movement alone, in the absence of any other actin nucleators. VASP functions as an actin *recruiter*, where its functionality relies on its ability to recruit preformed F-actin seeds via the FAB domain from the bulk solution and processively elongate them into long filaments. We find that cofilin promotes the nucleation of numerous F-actin seeds recruited by VASP, also under conditions where spontaneous actin nucleation is unfavorable, *i.e.* elevated profilin concentrations. VASP promotes filament elongation while competing with CPs, with an efficiency that depends on profilin concentration. Finally, the addition of an additional component such as methylcellulose or fascin is required for actin bundle formation and motility mediated by VASP.

EXPERIMENTAL PROCEDURES

Protein Purification—Actin was purified from rabbit skeletal muscle acetone powder (37) with a gel filtration step, stored on ice, and used within 2 weeks. His-VASPs (and constructs of VASP mutants) were produced as N-terminal His fusions as detailed previously (21). Recombinant GST-fascin was prepared by a modification of the method of Ono *et al.* (38). Human profilin was purified in the initial stage by capture to beads coupled to poly-L-proline and removed by urea followed by refolding and size exclusion. Human cofilin was purified by ammonium sulfate precipitation followed by size exclusion and ion exchange chromatography. Actin was labeled on Cys-374 with Alexa-Fluor 488 (Invitrogen) or Cy3 (Molecular Probes), according to standard protocols.

Cryo-transmission Electron Microscopy (Cryo-TEM)—Cryo-TEM was used to obtain high resolution information on the homogeneity of VASP distribution on the surface of the beads (Polysciences). Specimens for cryo-TEM were prepared according to a standard procedure (39). Samples were stored under liquid nitrogen before transfer to a TEM (Tecnai 12, FEI) operated at 120 kV in low-dose mode, with underfocus at a few micrometers to increase phase contrast. Images were recorded on a Gatan 794 or Gatan 791 CCD camera with Digital Micrograph software.

Bead Motility Assay—Polystyrene beads (Polysciences) (2.06 μm in diameter) were incubated in a solution consisting of 15 μM His-VASP constructs (WT VASP, VASP-ΔPro, or VASP-ΔFAB) for 30 min at room temperature. The surface of the beads was then passivated with a solution of 10% BSA according to the protocol detailed previously (40). All beads were used within 24 h. VASP-coated beads were immersed in a motility medium containing 10 mM Tris-HCl, pH 7.6, 1.7 mM Mg-ATP, 5.5 mM DTT, 15 μM glucose, 0.1 mg/ml glucose oxidase, 0.018 mg/ml catalase, 0.2 mM EGTA, 50 or 100 mM KCl, 1 mM $MgCl_2$, 1.1–1.65 μM Ca-ATP-actin (9.1% labeled with Alexa Fluor 488 and preincubated with profilin, when profilin is added), 0 or 20 nM CPs, 0–8 μM profilin, 0 or 2.5 μM human cofilin, and an actin bundling component, such as methylcellulose (MC) or fascin (55 nM). Replacing actin monomers with F-actin gave the same general behavior, *i.e.* growth of bundles and propulsion of beads. Yet quantitative analysis was only performed in assays done with actin monomers for which the concentration is known. For bead motility assays done in the presence of thymosin-β4 (tβ4) (ProSpecBio Ltd.), we used 1.1 μM Ca-ATP-actin (9.1% labeled with Alexa Fluor 488), 1 μM profilin, and 5 μM tβ4.

Samples were imaged within 10 min after mixing, by phase contrast and fluorescence microscopy using an Olympus IX-71 inverted microscope with a ×60 oil objective. The images and time-lapse were acquired using an Andor back illuminated DU-897 EMCCD camera controlled by Metamorph software (Molecular Devices).

FRAP Experiments—Fluorescent recovery after photobleaching (FRAP) experiments was used to measure the dynamics of actin at the tip of the bundle, in the vicinity of the bead, and along the bundle, away from the bead surface. FRAP experiments were done on a spinning disc confocal microscope (UltraView ERS FRET-H-System, PerkinElmer Life Sciences), based on an Axiovert-200 M microscope (Zeiss, Germany) equipped with a Plan-Neofluar ×63/1.4 oil objective and a Hamamatsu interline CCD camera (Hamamatsu C9100-50) driven by ImageSuite ERS. For the experiments, a spot area (spot size) of ~3 μm^2 was bleached (300 iterations at full laser power at 488 nm, argon source). Two pre-bleached frames were acquired at time intervals of 0.1 s between frames. Immediately after bleaching, the entire field was acquired at a scanning rate of 0.2 s per frame typically for 15 s and then at a rate of 30 s per frame. The two scanning rates were optimized for measuring the dynamics at short times (which is rapid and dominated by the diffusion of actin monomers into the bleached region) and at longer times (which is relatively slow and results from continuous polymerization of actin on the bead surface). The intensity of fluorescence recovery signal $I(t)$ was normalized according to $I(t) - I_0/I_{max} - I_0$, where I_{max} and I_0 are the intensities immediately before and after photobleaching, respectively.

Data Analysis, Bead Propulsion Velocity, and Bundle's Elongation Rate—The rate at which bundles grow from the surface of the beads is designated v_p, and the velocity of beads propelled by the action of a comet tail is designated as v. Measurement of the beads' propulsion velocity v was carried out on beads propelled by the action of a single actin tail. v_p and v were extracted by measuring the changes in the total length of the growing bundles or propelling tail with time. Typically, 5–10 beads (with 5–10 bundles per bead) were analyzed for each experimental condition. For the analysis, we manually measured changes in the actin bundle total length (dL_i) from the bead surface to the end of the bundle for a time interval (dt_i). The detailed analysis is based on Ref. 41. The error bars are standard deviations. Student's t tests were also applied (p values are indicated for values smaller than 0.05). Analysis of the experimental data

were performed using METAMORPH (Molecular Devices), Excel, and Origin (OriginLab Corp.).

Bundle Cross-section Intensity—The simplest way to estimate the number of filaments per bundle is to measure the bundle thickness. Yet most bundles are very thin (*i.e.* equal to or below resolution limits), such that measuring their thickness from fluorescence or phase contrast images is highly inaccurate. In contrast, the cross-section fluorescence can be measured accurately. For given illumination settings, camera gain, and percentage of labeled actin, the total fluorescence reflects the total number of filaments in that cross-section. Practically, the total fluorescence intensity is measured at a well defined distance from the bead surface (~5 μm). The logic for choosing this distance relies on the fact that it is, on one hand, far enough from the bead surface so that the measured fluorescence is the one emanating from the filaments, without being biased by the intensity emitted from the bead surface. On the other hand, this distance is sufficiently close to the bead surface to ensure that the measured fluorescence reflects the actual density of actin filaments that polymerize at the bead surface. Measuring the intensity farther away from the surface may give erroneous (lower) values due to possible disassembly of the actin bundle. For each experimental condition, we measured the cross-section intensity of 30–50 bundles. Measurements and analysis of the elongation rate, cross-section intensity, and bead velocity were done using METAMORPH (Molecular Devices), Excel, and Origin (OriginLab Corp.).

Single Actin Filament TIRF Assays—The protocol for total internal reflection fluorescence (TIRF) assay is based on Ref. 42. In experiments testing the effect of profilin and CPs, Ca-ATP-actin was first incubated with various concentrations of profilin (0–16.5 μM) in G-buffer (5 mM Tris-HCl, pH 7.8, 0.01% NaN_3, 0.1 mM $CaCl_2$, 0.2 mM ATP, 1 mM DTT) for 10 min at room temperature. In a following step, Ca-ATP-actin (15% labeled with Alexa Fluor 488 or Cy3) was converted to Mg-ATP-actin for each experiment by adding 1/10 part of 10× magnesium-exchange buffer (10 mM EDTA, 1 mM $MgCl_2$), to give the appropriate factor of the final actin concentration, and incubated on ice for 2–3 min.

Actin Filament Polymerization from Beads—In assays with beads, 1 volume (10 μl) of 2× Mg-ATP-actin (2.2 μM, 15% labeled with Cy3) preincubated with 2× profilin (0–33 μM) was mixed with 1 volume (10 μl) of 2× TIRF buffer (20 mM imidazole, pH 7.0, 100 mM KCl, 2 mM $MgCl_2$, 2 mM EGTA, 200 mM DTT, 0.4 mM ATP, 1% methylcellulose, 30 mM glucose, 40 μg/ml catalase, 200 μg/ml glucose oxidase). In these experiments, we used 0.5% (v/v) 2.06-μm diameter polystyrene microspheres (Polysciences) coated with 15 μM VASP according to the procedure used for the bead motility assays. 30 μl of the final solution was immediately loaded into a NEM-myosin-coated chamber and placed on the microscope.

Actin Nucleation in the Bulk Solution, Combined Effect of Cofilin and Profilin—We tested the effect of cofilin (0 or 2.5 μM) on actin nucleation in the absence (0 μM) and in the presence of 6 μM profilin. One volume (10 μl) of 2× Mg-ATP-actin (2.2 μM, 15% labeled with Alexa Fluor 488) preincubated with 2× profilin (0–12 μM), 100 mM KCl, and cofilin (0 or 5 μM) was mixed with 1 volume (10 μl) of 2× TIRF buffer. 30 μl of the final solution was immediately loaded into a NEM-myosin-coated chamber and placed on the microscope. For each experimental condition, images were taken every 10 s. Actin nucleation was determined by counting the number of actin filaments present at short (5 min) and long (25 min) times, using ImageJ software.

Actin Polymerization from Phalloidin-stabilized F-actin Seeds—Phalloidin-stabilized F-actin seeds were prepared by mixing (1:1 molar ratio) actin filaments with phalloidin (9.1% labeled with rhodamine (Invitrogen)) and incubating them at room temperature for 30 min. For experiments using VASP-capped F-actin seeds, we initially incubated 40 nM phalloidin-stabilized F-actin seeds with 40 nM VASP in F-buffer (5 mM Tris-HCl, pH 7.8, 0.01% NaN_3, 100 mM KCl, 1 mM $MgCl_2$, and 0.2 mM EGTA) for 15 min at room temperature. 15 μl of the solution was flowed into a NEM-myosin-coated chamber and incubated for additional 2 min.

For experiments done in the absence of CPs, 1 volume (10 μl) of 2× Mg-ATP-actin (1.5 μM, 15% labeled with Alexa Fluor 488) preincubated with 2× profilin (0–18 μM), 100 mM KCl, and 50 nM VASP was mixed with 1 volume (10 μl) of 2× TIRF buffer. Control experiments were carried out in the absence of VASP to measure bare filament elongation rates at the same profilin concentration. In the assays done with CPs, 1 volume (10 μl) of 4× Mg-ATP-actin (3 μM, 15% labeled with Alexa Fluor 488) preincubated with 4× profilin (0–36 μM) was mixed with 1 volume (10 μl) of 4× solution composed of 200 mM KCl, 4 nM CPs, 100 nM VASP, and 2 volumes (20 μl) of 2× TIRF buffer. The final solution was immediately loaded into the NEM-myosin-coated chamber containing phalloidin stabilized F-actin seeds and placed onto the microscope.

For each experimental condition, we followed the elongation of individual actin filaments growing from beads or F-actin seeds every 10 s, until overlapping between filaments was observed. When using F-actin seeds, for each profilin concentration the total length of typically 15 filaments was automatically tracked, using length measurements of the JFilament two-dimensional algorithm as plug-ins for ImageJ. The elongation rate v_p was extracted from the linear part of the total length *versus* time curve (41).

Total internal reflection fluorescence microscopy (TIRFM) experiments were carried out on a Leica DMI6000 B microscope. Samples were excited by total internal reflection illumination at 488 and 568 nm, and images were captured with an Andor back-illuminated DU-897 EMCCD camera controlled by Leica software (LAS-AF-6000, Leica Microsystems CMS GmbH, Germany).

RESULTS

VASP Promotes Actin-based Motility—Micron-sized beads were coated with 15 μM WT VASP molecules homogeneously distributed over the surface as confirmed by cryo-TEM (data not shown). The beads were added to a mixture of purified proteins consisting of actin, profilin, cofilin, CPs, and MC, which promote actin filament bundling (see under "Experimental Procedures") (43). 5–25 min after mixing (depending on experimental conditions), we observed the growth of numerous actin bundles from the surface of the beads (Fig. 1*A* and supplemental Movie 1), which sometimes fused to form thicker bun-

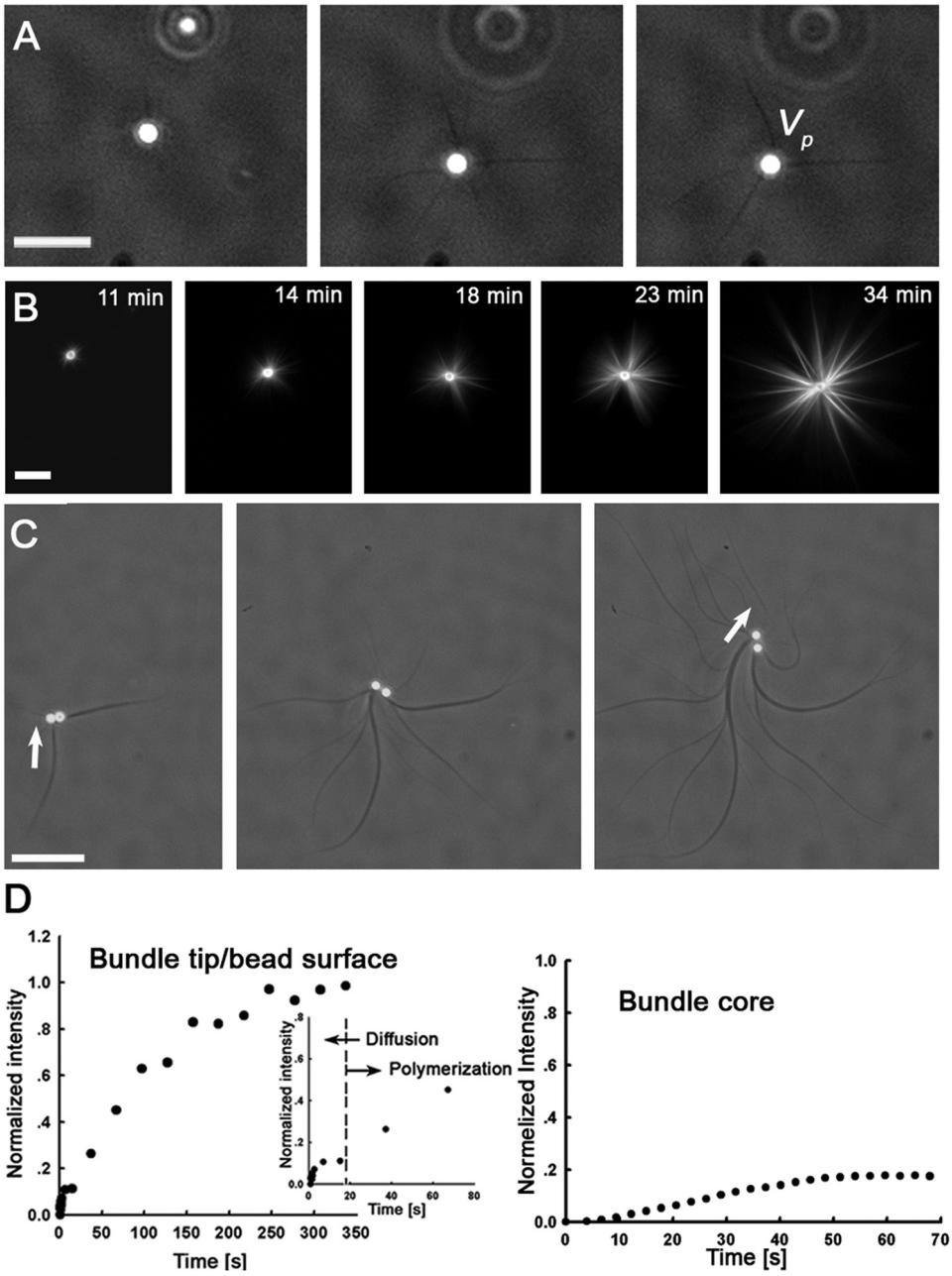

FIGURE 1. **VASP mediating the growth of actin bundles and motility of beads.** *A,* time-lapse (phase contrast) images of processive elongation of actin bundles from the surface of 15 μM WT VASP-coated beads. Conditions used are as follows: 7 μM F-actin, 5 μM profilin, 60 nM CPs, 5 μM cofilin, and 0.3% MC. The time difference between two sequential frames from *left to right* is $\Delta t = 18.33$ and 22.17 min. *Scale bar,* 10 μm. *B,* time-lapse fluorescence images of processive elongation of actin bundles from the surface of 15 μM WT VASP-coated beads. Conditions used are as follows: 1.1 μM Mg-ATP-actin, 6 μM profilin, 2.5 μM cofilin, and 55 nM fascin. *Scale bar,* 10 μm. *C,* time-lapse (phase contrast) images of 15 μM WT VASP-coated beads pushed by bundles that polymerize at the rear. The *arrow* marks the direction of movement. Conditions used are as follows: 7 μM F-actin, 10 μM profilin, 60 nM CPs, 5 μM cofilin, and 0.3% MC. Time difference between two sequential frames from *left to right* is $\Delta t = 25$ and 59 min. *Scale bar,* 20 μm. *D,* FRAP of actin fluorescence (normalized) at the bundle tip, *i.e.* in the vicinity of the bead (*left panel*), and far from the bead surface along the bundle core (*right panel*). The recovery signal at the bead surface divides to two as follows: (i) fast partial recovery of the fluorescence signal, which is attributed to the fraction of mobile actin monomers that diffuse inside the bleached region (*inset, Diffusion* zone); and (ii) a slow linear increase of the fluorescence signal, which is associated with the polymerization of actin (*inset, Polymerization*). The recovery signal away from the bead surface is partial and is attributed to the fraction of mobile actin monomers that diffuse inside the bleached region. Conditions used are as follows: 1.1 μM Mg-ATP-actin (9.1% Alexa Fluor 488-labeled), 6 μM profilin, 2.5 μM cofilin, and 0.3% MC.

dles (supplemental Movie 2). Bundles formed efficiently also in the presence of fascin, the characteristic bundling protein in filopodia (6). Numerous bundles grew from the surface of the beads, generating a dense array of straight bundles (Fig. 1*B*). In contrast to MC, we did not observe fusion of fascin bundles or motility, although the two phenomena are related because fusion promotes the breaking of the spherical symmetry, which is essential for motility (Fig. 1*C* and supplemental Movie 3).

Several observations led us to conclude that the barbed ends of the filaments in the bundles point toward the surface of the beads. The first observation is based on the fact that bundles that grew from the surface of the beads promoted the propul-

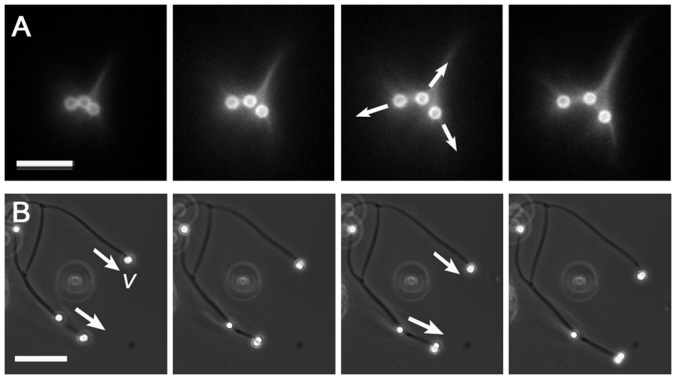

FIGURE 2. **Actin-based motility by VASP.** *A,* initial stage of the separation of a three-bead cluster mediated by the polymerization of actin on the surface of the beads. The *arrows* mark the direction of motion of the beads. Conditions used are as follows: 1.65 μM Mg-ATP-actin (9.1% Alexa Fluor 488-labeled), 6 μM profilin, 2.5 μM cofilin, and 0.3% MC. Time between frames from *left to right* is Δt = 4, 5, and 13 min. *Scale bar,* 10 μm. *B,* time-lapse (phase contrast) images of 15 μM WT VASP-coated beads at late stages, originally part of a four-bead cluster. The beads are propelled by the action of an actin tail polymerizing at the rear. The *arrows* mark the direction of movement. Conditions used are as follows: 7 μM F-actin, 5 μM profilin, 200 nM CPs, 5 μM cofilin, and 0.3% MC. Time between frames from *left to right* is Δt = 3.5, 5.5, and 7.67 min. *Scale bar,* 20 μm.

sion of beads (Fig. 1*C* and supplemental Movie 3). The second observation comes from FRAP experiments performed at different locations along the bundle (Fig. 1*D*), notably in the vicinity of the beads (Fig. 1*D*, *left panel*) and along the bundle, away from the bead surface (Fig. 1*D*, *right panel*). In the vicinity of the surface, the recovery of the fluorescence signal is initially fast and partial and is attributed to the diffusion of actin monomers into the bleached region (Fig. 1*D*, *inset* in *left panel*). It was followed by a slow recovery that grows linearly with time (Fig. 1*D*, *inset* in *left panel*), reflecting the continuous polymerization of actin at the bead surface. Full recovery was observed at the end of the process. A similar linear growth was observed for beads propelled by a branched actin tail, where the increase in fluorescence reflected the continuous polymerization of new actin branches at the bead surface (41). Along the bundle core, the recovery signal is partial and is attributed to the fraction of mobile actin monomers that diffuse inside the bleached region (Fig. 1*D*, *right panel*). Finally, the fact that the bundles are thinner at the extremity that points away from the bead surface suggests actin disassembly. We therefore conclude that the filaments' barbed ends are associated with the VASP molecules at the bead surface.

Beads coated with VASP tend to stick and form clusters. The size of the clusters can vary, from a few (Fig. 2, *A* and *B*) to tens of beads. As time elapsed, the beads that were initially in contact started to separate and moved away from each other (see for example the three-bead cluster in Fig. 2*A* and supplemental Movie 4). Eventually, beads that originated from small clusters ($\leq$3 beads) were propelled by the action of a single comet tail and moved at constant velocity v for ~1 h (Fig. 2*B* and supplemental Movie 5). The motion of clusters consisting of numerous beads ($\gg$3) was more complex, as in these cases the beads were propelled by several comets simultaneously (supplemental Movie 6). We compared the velocity v of moving beads with the growth rate of bundles v_p and found that they have very similar values (data not shown). This led us to conclude that a propelling tail and a growing bundle are equivalent objects such that the conclusions deduced from the analysis of growth of the bundles can be used for bead propulsion and vice versa.

Finally, we found that the VASP-driven motility described above is essentially dependent on the formation of actin bundles, which is the first required step toward breaking the spherical symmetry of the actin coat needed for motility. In Fig. 3, we demonstrated that there is a minimal concentration of MC below which there are no bundles. Moreover, we also show that the elongation rate of bundles is insensitive to the concentration of added MC. From that point on, all experiments were carried out at 0.3% MC.

VASP-coated Beads, Role of Profilin, Capping Proteins, and Cofilin on Bundle Formation, Growth, and Motility—The motility medium contained actin and accessory proteins implicated in actin nucleation and turnover, including profilin, CPs, and cofilin. The experiments were done at a physiological salt condition (100 mM KCl) for which VASP has no actin nucleation activity (21, 44). We investigated how each individual protein affected bundle formation and growth, as well as motility. The results are summarized in Fig. 4*A*. Our data show that bundles form and elongate from VASP-coated beads in the presence of actin alone, which suggests that neither profilin nor cofilin nor CPs are necessary for bundle formation and growth (Fig. 4, *A* and *B*).

We started by investigating the effect of profilin. Increasing the concentration of profilin did not significantly affect the formation of actin bundles up to 4 μM (Fig. 4*B*, *upper row*), whereas their ability to elongate was reduced at high profilin concentrations ($\geq$4 μM). The effect was even more significant when the concentration of profilin was further increased to 6 μM. At this concentration, the bundle formation was strongly suppressed. The system was now composed of short and diffuse bundles. Also, no motility of beads was observed.

We then investigated the combined effect of profilin and CPs. In the absence of profilin, numerous bundles formed in the presence of CPs (Fig. 4*B*, *middle row*), indicating that VASP efficiently competes with CPs for the barbed ends binding filaments, in accordance with previous studies (12, 21, 22, 24). The addition of profilin was found to affect bundle formation (Fig. 4*B, middle row*). For low concentrations of profilin, actin bundles formed without significant differences compared with the case where no profilin was added. However, the addition of 3 μM profilin totally inhibited bundle formation (instead, a diffuse layer of actin was formed), except for very rare cases (~5%) where thin bundles formed (data not shown). The total intensity of the actin layer gradually decreased with a further increase in profilin concentration; for 8 μM profilin, actin fluorescence was ~10-fold lower compared with the case with no profilin.

The strong reduction in system activity at high profilin concentrations was further investigated. At such a large molar excess of profilin over actin, the observed reduction in system activity may result from the binding to VASP of free profilin instead of profilin-actin complexes (13). At such large profilin concentrations, the spontaneous actin nucleation is also strongly suppressed (45). To discriminate between these two possible effects, we replaced profilin with tβ4, which is known

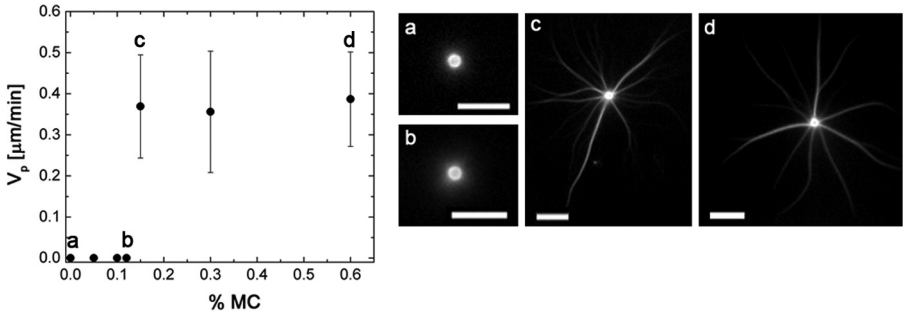

FIGURE 3. **Dependence of bundle formation and elongation rate on MC concentration.** *Left panel,* mean elongation rate of actin bundles as a function of MC concentration. Values correspond to mean ± S.D. Fluorescence images in the *right panel* show actin bundles polymerizing from the surface of 15 μM WT VASP-coated beads (*panel a*) in the absence of MC, (*panel b*) 0.12%, (*panel c*) 0.15%, and (*panel d*) 0.3% MC, as labeled on the graph. Conditions used are as follows: 1.1 μM Mg-ATP-actin (9.1% Alexa Fluor 488-labeled), 6 μM profilin, 20 nM CPs, and 2.5 μM cofilin. *Scale bar,* 10 μm.

A

Composition	Actin layer on surface	Formation of bundles	Elongation	Bead movement
Actin alone	+	+	+	----
Actin+Profilin	+	+	+	----
Actin+CPs	+	+	+	----
Actin+CPs+Profilin (0.1μM)	+	+	+	----
Actin+CPs+Profilin (3μM)	+	-(very weak)	----	-
Actin+CPs+Profilin (6μM)	+	-(very weak)	----	-
Actin+CPs+Profilin (8μM)	-(very weak)	-	-	-
Actin+Cofilin	+	+	+	----
Actin+Cofilin+CPs	+	+	+	+
Actin+Cofilin +Profilin (6μM)	+	+	+	+
Actin+Cofilin+CPs+Profilin(6μM)	+	+	+	+

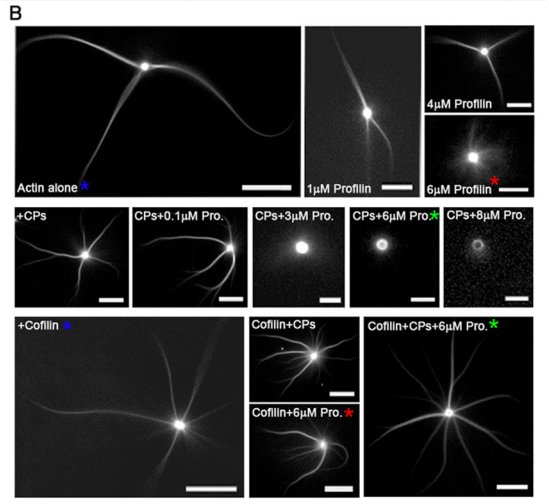

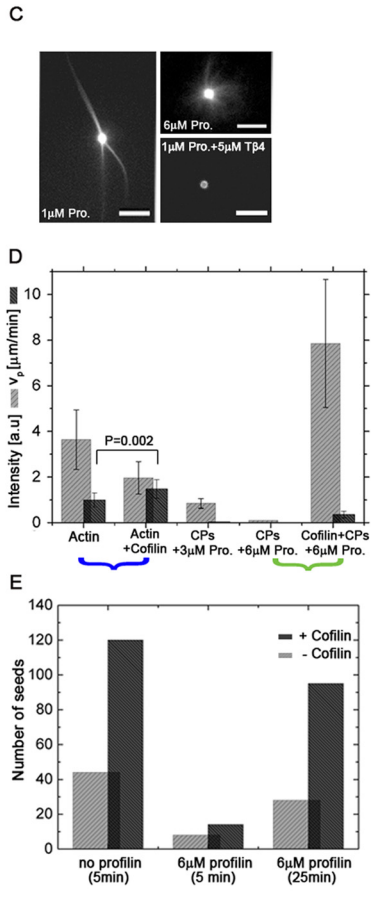

FIGURE 4. **Motility and bundle formation from WT VASP-coated beads at different compositions of the motility medium.** *A, table* summarizes the effect of profilin, cofilin, and CPs on bead motility and bundle formation and growth. The scores +, −, and — refer to observed, not observed, and not determined, respectively. *B,* fluorescence images of 15 μM WT VASP-coated beads immersed in the motility medium for 1 h. *Top,* effect of profilin concentration: *left to right,* 0 (actin alone, *blue asterisk*, *scale bar,* 20 μm); 1 μM (*scale bar,* 10 μm); 4 μM (*scale bar,* 10 μm); and 6 μM profilin (*red asterisk*, *scale bar,* 10 μm). Conditions used are as follows: 1.1 μM Mg-ATP-actin (9.1% Alexa Fluor 488-labeled), and 0.3% MC. *Middle,* effect of profilin concentration in the presence of CPs: *left to right,* 0 (CPs alone, *scale bar,* 10 μm); 0.1 μM (*scale bar,* 10 μm), 3 μM (*scale bar,* 5 μm), 6 μM (*green asterisk, scale bar,* 5 μm), and 8 μM profilin (*scale bar,* 5 μm). Conditions used are as follows: 1.1 μM Mg-ATP-actin (9.1% Alexa Fluor 488-labeled), 0.3% MC, and 20 nM CPs. *Bottom,* effect of cofilin: fluorescence images of actin bundles in the presence of 2.5μM cofilin (*blue asterisk, scale bar,* 20 μm); 2.5 μM cofilin and 20 nM CPs (*scale bar,* 10 μm); 2.5 μM cofilin and 6 μM profilin (*red asterisk*, *scale bar,* 10 μm); and 2.5 μM cofilin, 20 nM CPs, and 6 μM profilin (*green asterisk, scale bar,* 10 μm). Conditions used are as follows: 1.1 μM Mg-ATP-actin (9.1% Alexa Fluor 488-labeled), and 0.3% MC. *C,* fluorescence images of 15 μM WT VASP-coated beads in the presence of profilin or profilin and tβ4. *Scale bar,* 10 μm. *D,* comparison of the mean fluorescence intensity of actin bundles' cross-section and mean elongation rate for conditions with and without cofilin; cofilin was added to a pure actin solution (*blue brace*) and to a solution of actin, CPs, and 6 μM profilin (*green brace*). *Numbers* on the top of *bars* indicate *p* values whenever the difference in elongation rate was significant ($p < 0.05$). *E,* cofilin-mediated F-actin seed nucleation in the absence or in the presence of high concentrations of profilin. The number of F-actin seeds formed at short and long times is given.

to prevent spontaneous actin nucleation and sequester actin monomers (46) but not to interact with VASP. We used 1 μM profilin and added 5 μM tβ4. Because tβ4 and profilin can exchange monomers (47), polymerization of profilin-actin complexes would still proceed with low profilin concentrations yet nucleation in the bulk could still be prevented. The experiments were done in the absence of CPs to prevent any blocking of actin polymerization at the bead surface. The addition of tβ4

suppressed system activity (Fig. 4*C*). Only very weak fluorescence was observed on the bead surface, and no bundles were formed. Our data thus show that even under conditions that favor filament elongation, bundle formation and motility are lost when actin nucleation is prevented in the bulk solution. From these experiments, we also conclude that a large molar excess of profilin strongly reduces *de novo* nucleation of F-actin seeds in the bulk, which is needed to initiate bundle formation rather than blocking the proline-rich domain of VASP.

In contrast to profilin, the addition of micromolar cofilin concentration (2.5 μM) to the motility medium had a positive effect on system activity. First, regardless of the motility medium composition, the beads were motile in the presence of cofilin (Fig. 4*A*). Second, the addition of cofilin to a pure actin solution or to a solution of actin and CPs (Fig. 4*B*, *bottom row*) induced the formation of more bundles (approximately twice) in comparison with a system lacking cofilin (Fig. 4*B*, *upper row*). The bundles were thinner (*i.e.* had lower cross-section intensity) and elongated faster (Fig. 4*D*, *blue brace*). The faster velocity may arise from two possible mechanisms as follows: (i) lower depletion of actin monomers due to lower overall number of filaments (more bundles but much thinner), or (ii) binding of cofilin along the backbone of the filaments, proposed to occur at micromolar concentrations (48), reduces the binding strength of the VASP molecules to the side of the growing filaments, overall promoting faster elongation rates. A similar argument was used to explain the increase in velocity of beads propelled by the action of a branched actin tail (41, 49).

Finally, against the negative effects observed at high profilin concentrations, the addition of cofilin rescued motility and bundle formation, with or without CPs (Fig. 4*B*, *green* and *red asterisks*, respectively and Fig. 4*D*, *green brace*). Repeating the experiments at 50 mM KCl showed a certain improvement in the ability of the system to generate actin bundles (~15% of the beads formed 1–2 bundles, whereas 85% of the beads generated diffused actin bundles similarly to those formed with 100 mM KCl), which is in accord with the fact that VASP nucleates actin at nonphysiological salt concentrations (44, 50). Nevertheless, none of the beads were motile. Moreover, and similarly to the results observed at physiological salt conditions, the addition of cofilin rescued bundle formation and motility. Our data suggest that actin nucleation efficiency of VASP at high profilin concentrations is too low to support bead motility and bundle formation, regardless of salt concentration. The fact that the beads are motile and grow numerous bundles in the presence of micromolar concentrations of cofilin suggests that cofilin enables actin nucleation even at high profilin concentrations, where spontaneous actin nucleation is strongly suppressed.

To correlate between bundle formation by VASP and cofilin-mediated F-actin seed formation in the bulk, we examined the ability of cofilin to promote actin nucleation in the absence and in the presence of high concentrations of profilin using TIRF microscopy. The concentrations of profilin and cofilin were the same as those used in the bead motility assay. In the absence of profilin, the addition of micromolar concentrations of cofilin (2.5 μM) increased the number of F-actin seeds nucleated in the bulk (Fig. 4*E*), in accord with a previous study (48). Numerous F-actin seeds were nucleated within a few minutes (~5 min),

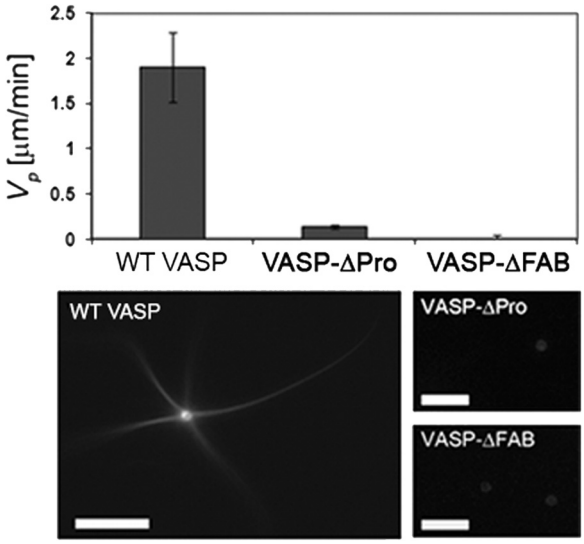

FIGURE 5. **Polymerization of actin bundles on beads coated with different VASP constructs.** Comparison of bundle elongation rates of beads coated with 15 μM WT VASP, VASP-ΔPro, and VASP-ΔFAB. Values correspond to mean ± S.D. Fluorescence images of actin bundles polymerizing (9.1% labeled with Alexa Fluor 488) from beads coated with 15 μM WT VASP, VASP-ΔPro, and VASP-ΔFAB mutants; images were taken 25, 49, and 43 min after mixing, respectively. Conditions used are as follows: 1.65 μM Mg-ATP-actin, 6 μM profilin, 2.5 μM cofilin, and 0.3% MC. *Scale bar,* 20 μm (WT VASP) and 10 μm (VASP-ΔPro and VASP-ΔFAB).

which also corresponded to the time when bundles started to form on the beads (Fig. 4*B*, *upper row*). We also examined the ability of cofilin to nucleate actin at high concentrations of profilin (6 μM). At short times, cofilin increased the number of F-actin seeds nucleated in the bulk but not significantly in comparison with a solution lacking cofilin (Fig. 4*E*). However, after 20–25 min, which corresponds to the time when bundles started to form on the beads, we measured an ~6-fold increase in the number of F-actin seeds, which is similar to the number of F-actin seeds produced after ~5 min in the system lacking profilin (Fig. 4*E*). This means that in the presence of high concentrations of profilin, F-actin seed nucleation by cofilin is delayed but not inhibited. Overall, our data show that there is a tight correlation between F-actin seed production in the solution and bundle formation by VASP. Bundle formation by VASP is regulated by the concentration of F-actin seeds produced in the bulk such that bundles start to form when the concentration of seeds exceeds a concentration threshold.

VASP Mutants Coated on Beads, FAB Domain Is Indispensable for Actin-based Activity by VASP—Our data suggest that bundle growth and motility by VASP are initiated by the recruitment of F-actin seeds from the solution to the bead surface and their subsequent elongation by the recruitment and transfer of profilin-actin complexes to the filament barbed end. To reveal the importance of the FAB and proline-rich domains for VASP function, we used two mutants as follows: VASP-ΔFAB that lacks the F-actin-binding motif and VASP-ΔPro that lacks the proline-rich domain responsible for recruiting profilin-actin complexes. The experiments were done in the presence of 6 μM profilin and 2.5 μM cofilin but in the absence of CPs to prevent the blocking of filament growth. Under these conditions, WT VASP induced the growth of numerous bundles from the surface of the beads (Fig. 5). The deletion of the

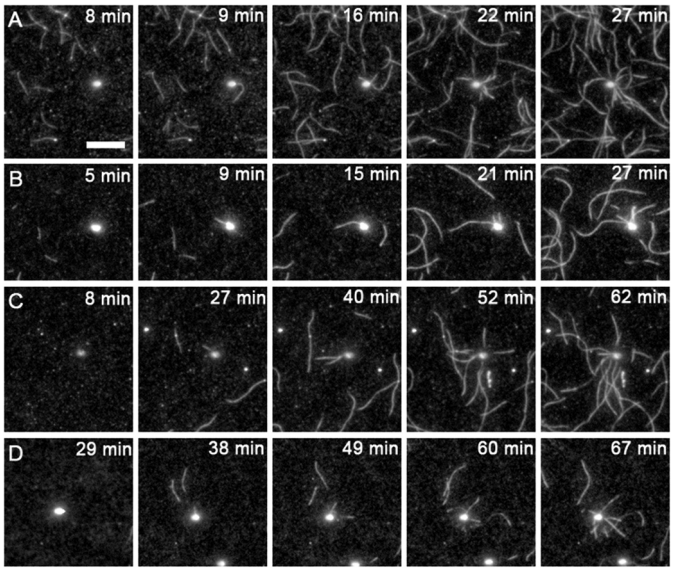

FIGURE 6. **Effect of profilin concentration on the polymerization of actin filaments in the bulk and from VASP-coated beads.** TIRFM image sequences showing filament nucleation and growth in the bulk and from the beads' surfaces. Conditions used are as follows: 1.1 μM Mg-ATP-actin (15% labeled with Cy3); *A,* 0; *B,* 1.1 μM; *C,* 6.6 μM, and *D,* 16.5 μM profilin. Indicated are times after mixing. *Scale bars,* 10 μm.

FAB or the proline-rich domains led to dramatic effects. Replacing WT VASP with VASP-ΔPro rendered most of the beads (>95%) inactive. The very few beads that grew bundles did so very inefficiently with $v_{p,\,\mathrm{VASP\text{-}\Delta Pro}}/v_{p,\,\mathrm{WT\ VASP}} = 0.075$; also, VASP-ΔPro did not produce any bead movement. Replacing WT VASP with VASP-ΔFAB was even more dramatic, abolishing motility and the formation and growth of actin bundles. Overall, the data show that both the FAB and the proline-rich domains are essential for the activity of VASP, although the deletion of the FAB domain is much more significant, rendering VASP essentially inactive.

Polymerization of Individual Actin Filaments from VASP-coated Beads in the Presence of Increasing Concentrations of Profilin—Our bead assay experiments have shown that the recruitment of the profilin-actin complex via the proline-rich domain is important for VASP function. Our next goal was to investigate how profilin influences bundle elongation rate. However, because bundles did not form at high concentrations of profilin, we could not measure the elongation rate of bundles under such conditions.

We overcame this problem by employing TIRF microscopy. This technique is extremely sensitive and allows the visualization of individual actin filaments growing from the surface of beads. It is also optimal for conditions where actin nucleation is very weak and only a few filaments grow from the surface. We followed the growth of individual actin filaments from the surface of the beads for a wide profilin concentration range (0–16.5 μM) (Fig. 6 and supplemental Movies 7–10). The elongation rates never exceeded the value measured with no profilin and decreased with the increase in profilin concentration (data not shown). The fact that we did not see any improvement, even at low profilin concentrations, was surprising. Generally, the formation of actin filaments in the bulk preceded the growth of filaments on the surface of the beads. Increasing profilin concentration gradually decreased the number of filaments that nucleated in the bulk and that grew from the surface of the beads (Fig. 6, *A–D*). The decrease in actin nucleation in the bulk with the increase in profilin concentration is in accord with our results (Fig. 4*E*) and biochemical assays (45). Thus, even though we could follow the growth of individual filaments from the surface of the beads and measure their elongation precisely, we could not compare the elongation rates measured at different profilin concentrations. The main reason for this comes from the fact that actin nucleation and growth in the bulk solution compete with that on the surface of the beads. Moreover, their relative importance depends on the concentration of added profilin. At low profilin concentrations, spontaneous actin nucleation in the bulk was very efficient, and numerous filaments elongated there before filament growth was observed on the surfaces of the beads, such that the concentration of actin monomers available for polymerization on the surface was reduced. This can explain the decrease in the elongation rates observed at low profilin concentrations. In contrast, at high profilin concentrations spontaneous nucleation of actin in the bulk was strongly reduced, and only a very few filaments grew in the bulk before filaments grew on the surface such that the concentration of free monomers available for polymerization on the surface was higher in comparison with that at low profilin concentrations. Because the elongation rate is controlled by the concentration of free monomers, comparing the elongation rates obtained at different profilin concentrations was not possible.

Effect of Profilin on the Polymerization of Actin from Phalloidin-stabilized F-actin Seeds—To eliminate the problem of filament nucleation, we decided to use F-actin seeds. The use of F-actin seeds enabled us to compare quantitatively the effect of profilin concentration on individual filament elongation rates v_p (Fig. 7). Several previous TIRF studies observed contradictory results regarding the effect of profilin on VASP-mediated elongation of individual filaments. One report reached the conclusion that profilin has no effect on the rate of filament elongation (23). Hansen and Mullins (12) found that profilin increases filament elongation rate, whereas Pasic *et al.* (22) observed the opposite effect. To shed light on the profilin effect on VASP function, we extended the concentration range studied from 75 nM to 9 μM profilin. We used TIRFM to measure the growth of actin (Alexa Fluor 488-labeled) from phalloidin-stabilized F-actin seeds (rhodamine-labeled) in the presence of 25 nM WT VASP, with different quantities of profilin (Fig. 7*A*). As a control, we used bare F-actin seeds and measured their elongation rate in the absence of VASP. In the absence of profilin, the elongation rate of VASP-capped seeds $v_{p,0}^{\mathrm{Vasp}} = 0.86 \pm 0.08$ μm/min is the same as that of bare F-actin seeds $v_{p,0}^{\mathrm{bare}} = 0.88 \pm 0.08$ μm/min, in accord with previous results (22). Considering a rate constant of 8 $\mu\mathrm{M}^{-1}\,\mathrm{s}^{-1}$ and unlabeled actin concentration (51), we estimate the elongation rate to be 0.89 μm/min, as we find experimentally. Except for very low concentrations of profilin (<375 nM profilin), filaments elongated up to 50% faster in the presence of VASP than without it (bare F-actin seeds), suggesting that VASP positively influences filament elongation rate (Fig. 7*A*). Also, in the presence of VASP, we observed a nontrivial variation of the elongation rate on profilin concen-

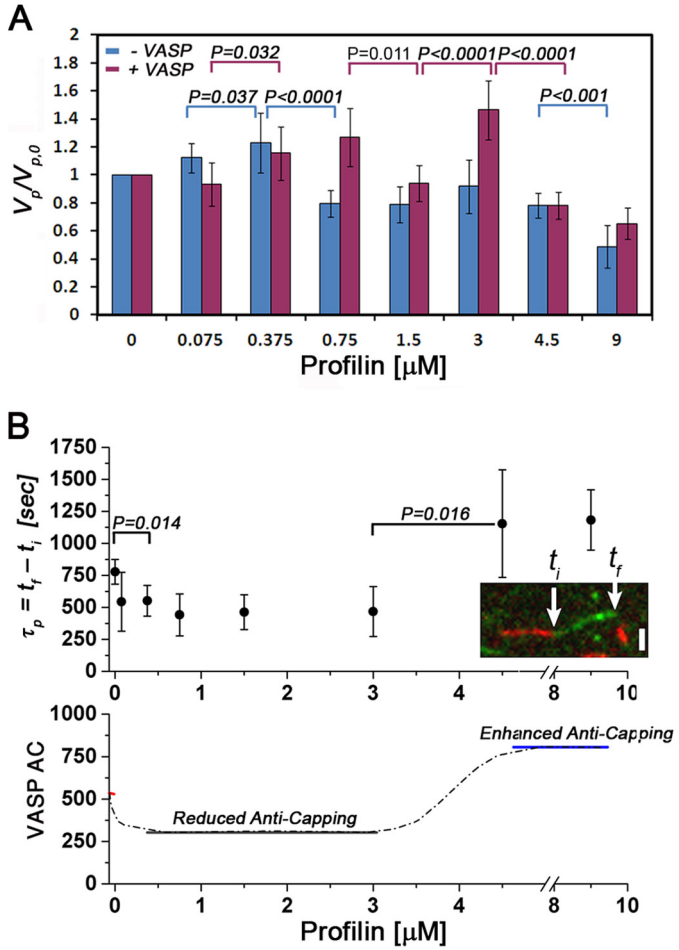

FIGURE 7. **Profilin concentration effect on filament elongation rate and VASP anti-capping activity.** *A,* normalized elongation rate $v_p/v_{p,0}$ as a function of profilin concentration for bare F-actin seeds and for WT-VASP-coated F-actin seeds in the presence of 25 nM solubilized VASP. All values correspond to mean ± S.D. *Numbers* on the top of *bars* indicate *p* values whenever the differences were significant ($p < 0.05$). Conditions used are as follows: 0.75 μM Mg-ATP-actin (15% labeled with Alexa Fluor 488). *B, top,* time to capping $\tau_p = t_f - t_i$ as a function of profilin concentration (t_i and t_f are the initial and final times of filament elongation, see image; *scale bar,* 5 μm). *Bottom,* number of VASP tetramers that attach/detach from the filaments' barbed ends until capping (defined as VASP AC) as a function of profilin concentration. Three regimes are observed as follows: *horizontal lines* mark the mean value of VASP AC in each of these regimes; *red line* marks the value of VASP AC in the absence of profilin; *black line* for 0.375 μM < [profilin] ≤3 μM; and the *blue line* corresponds to 4.5 μM < [profilin] ≤9 μM. All values correspond to mean ± S.D. *Numbers* on the top of *bars* indicate *p* values whenever the differences was significant ($p < 0.05$). Conditions used are as follows: 0.75 μM Mg-ATP-actin (15% labeled with Alexa Fluor 488), 25 nM WT VASP, and 1 nM CPs.

tration, which could be complicated because of VASP-profilin interactions (13, 14). Nevertheless, the general trend is that up to 3 μM profilin, the elongation rate increased with the increase in profilin concentration, exceeding the rates observed with actin alone. Above 3 μM profilin, the elongation rates decreased with the increase in profilin concentration, and they were slower than the values measured with no profilin, in accord with Pasic *et al.* (22). For bare F-actin seeds (*i.e.* without VASP), the elongation rate decreased with the increase in profilin concentration, except at very low profilin concentrations (<0.375 μM). The strong reduction in the elongation rates observed at high concentrations of profilin is in accord with previous studies (22, 45).

Profilin Dependence of the Anti-capping Activity of VASP—Anti-capping is associated with the ability of VASP molecules to compete with CPs for barbed end attachment and delay capping, overall resulting in a higher total amount of polymerized actin (21, 24) and longer filaments (12, 22). At the single filament level, the increase in filament length can result from the following: (i) the ability of VASP to compete with CPs for barbed end attachment and delay the time until capping (which is a measure of VASP AC activity); (ii) enhanced filament elongation rate v_p, or (iii) both. The effect of profilin concentration has not been studied at the single filament level, only in bulk pyrene assays (21).

We use TIRFM to measure the growth of actin (Alexa Fluor 488) from rhodamine phalloidin-stabilized F-actin seeds in the presence of WT VASP (25 nM), CPs (1 nM), and increasing amounts of profilin (0–9 μM). Bare F-actin seeds do not elongate in the presence of CPs (data not shown), even if VASP molecules are in the solution. This suggests that the affinity of CPs for free barbed ends is much greater than that of WT VASP (52, 53). VASP-capped F-actin seeds elongated continuously in the absence of CPs (data not shown), but in the presence of CPs the elongation plateaus after a certain time t_f (see image in Fig. 7*B*). This suggests that the binding of CPs is delayed in the presence of VASP, in accord with previous studies (12, 22, 24). The time it takes for the filaments to get capped and stop elongating is characterized by $\tau_p = t_f - t_i$, where t_i is the initial time of elongation. Under our experimental condition, τ_p is of the order of several minutes (Fig. 7*B, upper plot*). VASP AC activity is the ability of VASP molecules to compete with CPs for barbed end attachment, and it reflects the number of VASP molecules that associate/dissociate reversibly from the filament barbed end before a CP molecule binds irreversibly and terminates the elongation process. We can calculate this number by dividing τ_p by k_{off}^{-1}, the association time of a single WT VASP tetramer to the filament barbed end. Because VASP barbed end association time is independent of profilin concentration (12), the same value of $k_{off}^{-1} = 1.45$ s was used for all concentrations of profilin tested. For our experimental conditions, there are hundreds of VASP binding/unbinding events before capping occurs (Fig. 7*B, bottom plot*). The effect of profilin on τ_p and VASP AC shows that up to 3 μM, profilin has a negative effect on VASP AC. We observed an ~40% decrease in τ_p (and VASP AC) compared with a solution lacking profilin. A positive effect of profilin on VASP AC was observed above 3 μM. In that case, τ_p and VASP AC were larger by ~50% in comparison with a solution lacking profilin.

DISCUSSION

The mechanism by which VASP mediates actin-based movement is addressed in this work for the first time. Using a biomimetic bead assay, we show that VASP can promote actin-driven motility without the need of any additional (potent) actin nucleators. In this study, we combine bead motility and single filament TIRF assays to investigate VASP function in actin nucleation, filament growth, bundle formation and elongation, and motility in the presence of different actin regulatory proteins implicated in actin turnover. We systematically investigate the role of profilin, CPs, and cofilin alone and in admixture

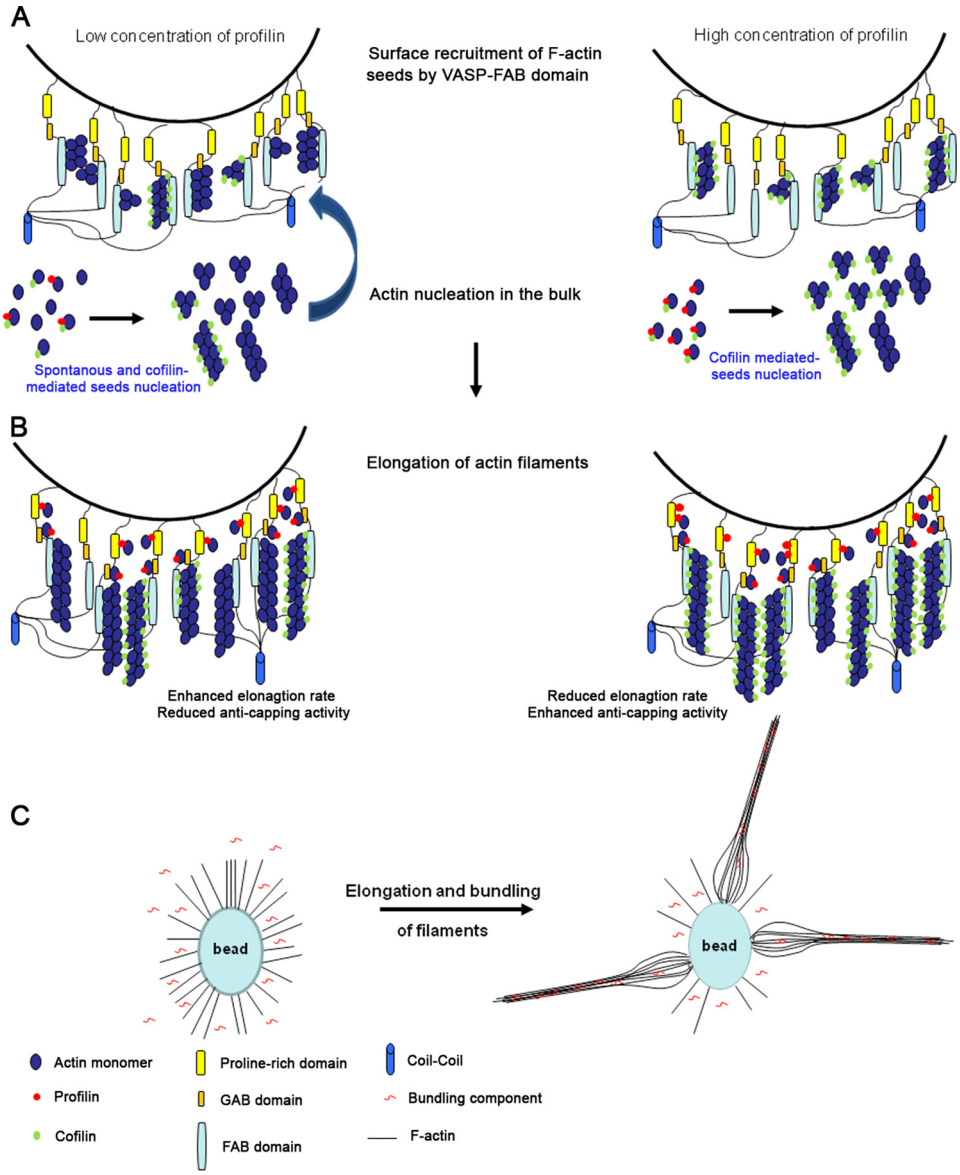

FIGURE 8. **Mechanism of actin-based motility by VASP, roles of profilin and cofilin.** *A* and *B,* bead coated with VASP molecules in the presence of micromolar concentrations of cofilin at low (*left panel*) and high (*right panel*) concentrations of profilin. *A,* recruitment of F-actin seeds from the bulk solution via VASP FAB domain to the surface of the beads. At low profilin concentrations, F-actin seed formation in the bulk solution occurs via spontaneous actin nucleation and cofilin-mediated actin nucleation. High profilin concentrations inhibit the spontaneous nucleation of actin in the bulk, thereby the majority of the F-actin seeds are produced by cofilin. *B,* filament elongation and anti-capping activity by VASP. VASP molecules promote processive elongation of unbranched actin filaments by association of profilin-actin complexes to the proline-rich domain, which are then transferred to the filament barbed end via VASP GAB domain, while remaining attached to the filament's side via VASP FAB domain. Enhanced (reduced) elongation rates and reduced (enhanced) VASP AC activity are observed for low (high) profilin concentrations, respectively. *C,* bundle formation depends on filament length. Transition from individual filaments to bundles occurs above a certain filament length for which the energy penalty associated with filament bending is compensated by the energy gain associated with their bundling.

to study their individual and combined effects on VASP function.

Our data show that at physiological salt conditions VASP nucleation activity is too weak to support motility and bundle formation. Rather, VASP functions as an actin *recruiter*, where its functionality relies on its ability to recruit F-actin seeds from the bulk solution and elongate them processively while competing with CPs with an efficiency that depends on profilin concentration (Fig. 8). We find that an additional component such as methylcellulose or fascin is required for actin bundle formation and motility mediated by VASP. Bundling occurs only if the filaments elongate enough that the elastic energy penalty associated with their bending is compensated for by the energy gain associated with their bundling (Fig. 8). The same type of argument was used to explain the transition from branched network to actin bundles (54–56).

The functional activity of VASP is initiated by the recruitment of F-actin seeds by the VASP-FAB domain, which is also important for processive filament elongation (12) and for the transformation of actin polymerization into motion. Our data show that VASP promotes motility and bundle formation only if sufficient F-actin seeds are produced in the bulk solution. We find that high concentrations of cofilin

promote the nucleation of numerous F-actin seeds even at high concentrations of profilin, which is needed in cells to minimize uncontrolled spontaneous nucleation in the bulk. Our data are consistent with *in vivo* studies demonstrating that high concentrations of active cofilin at the leading edge stimulate actin assembly and motility in carcinoma cells (57). The necessity for seeds for the initiation of branched network formation by the Arp2/3 complex was also shown *in vitro* both experimentally and theoretically (56, 58), and it is consistent with the fact that freshly polymerized actin is preferred for dendritic nucleation by the Wiskott-Aldrich syndrome protein-Arp2/3 complex (59). We thus suggest that cofilin functions at the cell's leading edge as an F-actin seed supplier by nucleating fresh polymerized actin recruited by VASP and Wiskott-Aldrich syndrome protein-Arp2/3 complex at the cell's leading edge of motile cells (24, 29, 57, 59, 60) and in neuronal systems (33, 36). We argue that the production of F-actin seeds in the bulk solution in cells does not contradict the requirement that uncontrolled filament assembly should be minimized. In fact, F-actin seeds that are not recruited at the cell leading edge are rapidly capped by CPs (which also localize to the cell leading edge (28)) and are depolymerized to refill the pool of actin monomers. In that way, network formation is regulated, and uncontrolled filament growth is minimized.

Following the recruitment of F-actin seeds, VASP promotes the elongation of filaments, while competing with CPs for barbed end attachment. Here, we show that the ability of VASP to compete with CPs depends on the concentration of profilin. At low/intermediate profilin concentrations, profilin enhances the elongation rate and reduces VASP anti-capping activity, while at high concentrations of profilin, we observe the opposite effects. This behavior can be explained as follows: at low/intermediate profilin concentrations, profilin-actin complexes are the major components in solution, whereas at high profilin concentration there is free profilin. We found that profilin concentration determines the affinity of VASP to actin filaments. At low/intermediate profilin concentrations, this affinity is weak, which allows both actin monomers and CPs to have easier access to the filament's barbed ends, thereby resulting in a higher elongation rate and reduced AC activity. However, at high profilin concentrations, the affinity of VASP to the filament barbed ends is high, resulting in lower accessibility of actin monomers and CPs to the barbed ends, thereby giving lower elongation rates and higher AC activity. In light of these results, and because the concentration of profilin in cells is elevated, we conclude that it is likely that *in vivo* VASP functions as a good anti-capper at the expense of reduced elongation rates. Therefore, VASP provides cells with the ability to grow persistent extensions, which grow continuously (but at a moderate rate) and do not undergo erratic movements and retractions. Such extensions are useful for many cell types and can explain the observed accumulation of Ena/VASP proteins in protruding lamellipodia (28) and at the tips of filopodia (5, 61, 62), where they efficiently compete with CPs.

Acknowledgments—A. B.-G. is grateful to D. A. Schafer for kindly providing the WT VASP and the two mutants VASP-ΔFAB and VASP-ΔPro. We thank Dr. Shira Albeck and Dr. Tamar Unger for the purification of WT VASP, VASP mutants, profilin, and cofilin. We thank Tom Pollard, Roberto Dominguez, and Cecile Sykes for useful comments and discussions. We also thank Nir Gov for careful reading of the manuscript and useful comments.

REFERENCES

1. Chakraborty, T., Ebel, F., Domann, E., Niebuhr, K., Gerstel, B., Pistor, S., Temm-Grove, C. J., Jockusch, B. M., Reinhard, M., and Walter, U. (1995) A focal adhesion factor directly linking intracellularly motile *Listeria* monocytogenes and *Listeria ivanovii* to the actin-based cytoskeleton of mammalian cells. *EMBO J.* **14,** 1314–1321
2. Laurent, V., Loisel, T. P., Harbeck, B., Wehman, A., Gröbe, L., Jockusch, B. M., Wehland, J., Gertler, F. B., and Carlier, M. F. (1999) Role of proteins of the Ena/VASP family in actin-based motility of *Listeria* monocytogenes. *J. Cell Biol.* **144,** 1245–1258
3. Loisel, T. P., Boujemaa, R., Pantaloni, D., and Carlier, M. F. (1999) Reconstitution of actin-based motility of *Listeria* and *Shigella* using pure proteins. *Nature* **401,** 613–616
4. Bear, J. E., Loureiro, J. J., Libova, I., Fässler, R., Wehland, J., and Gertler, F. B. (2000) Negative regulation of fibroblast motility by Ena/VASP proteins. *Cell* **101,** 717–728
5. Tokuo, H., and Ikebe, M. (2004) Myosin X transports Mena/VASP to the tip of filopodia. *Biochem. Biophys. Res. Commun.* **319,** 214–220
6. Adams, J. C. (2004) Roles of fascin in cell adhesion and motility. *Curr. Opin. Cell Biol.* **16,** 590–596
7. Drees, F., and Gertler, F. B. (2008) Ena/VASP: proteins at the tip of the nervous system. *Curr. Opin. Neurobiol.* **18,** 53–59
8. Lanier, L. M., Gates, M. A., Witke, W., Menzies, A. S., Wehman, A. M., Macklis, J. D., Kwiatkowski, D., Soriano, P., and Gertler, F. B. (1999) Mena is required for neurulation and commissure formation. *Neuron* **22,** 313–325
9. Wills, Z., Marr, L., Zinn, K., Goodman, C. S., and Van Vactor, D. (1999) Profilin and the Abl tyrosine kinase are required for motor axon outgrowth in the *Drosophila* embryo. *Neuron* **22,** 291–299
10. Lacayo, C. I., Pincus, Z., VanDuijn, M. M., Wilson, C. A., Fletcher, D. A., Gertler, F. B., Mogilner, A., and Theriot, J. A. (2007) Emergence of large-scale cell morphology and movement from local actin filament growth dynamics. *PLoS Biol.* **5,** e233
11. Pollard, T. D., and Borisy, G. G. (2003) Cellular motility driven by assembly and disassembly of actin filaments. *Cell* **112,** 453–465
12. Hansen, S. D., and Mullins, R. D. (2010) VASP is a processive actin polymerase that requires monomeric actin for barbed end association. *J. Cell Biol.* **191,** 571–584
13. Ferron, F., Rebowski, G., Lee, S. H., and Dominguez, R. (2007) Structural basis for the recruitment of profilin–actin complexes during filament elongation by Ena/VASP. *EMBO J.* **26,** 4597–4606
14. Chereau, D., and Dominguez, R. (2006) Understanding the role of the G-actin-binding domain of Ena/VASP in actin assembly. *J. Struct. Biol.* **155,** 195–201
15. Samarin, S., Romero, S., Kocks, C., Didry, D., Pantaloni, D., and Carlier, M. F. (2003) How VASP enhances actin-based motility. *J. Cell Biol.* **163,** 131–142
16. Plastino, J., Olivier, S., and Sykes, C. (2004) Actin filaments align into hollow comets for rapid VASP-mediated propulsion. *Curr. Biol.* **14,** 1766–1771
17. Trichet, L., Campàs, O., Sykes, C., and Plastino, J. (2007) VASP governs actin dynamics by modulating filament anchoring. *Biophys. J.* **92,** 1081–1089
18. Suei, S., Seyan, R., Noguera, P., Manzi, J., Plastino, J., and Kreplak, L. (2011) The mechanical role of VASP in an Arp2/3-complex-based motility assay. *J. Mol. Biol.* **413,** 573–583
19. Skoble, J., Auerbuch, V., Goley, E. D., Welch, M. D., and Portnoy, D. A.

(2001) Pivotal role of VASP in Arp2/3 complex–mediated actin nucleation, actin branch-formation, and *Listeria monocytogenes* motility. *J. Cell Biol.* **155,** 89–100
20. Trichet, L., Sykes, C., and Plastino, J. (2008) Relaxing the actin cytoskeleton for adhesion and movement with Ena/VASP. *J. Cell Biol.* **181,** 19–25
21. Barzik, M., Kotova, T. I., Higgs, H. N., Hazelwood, L., Hanein, D., Gertler, F. B., and Schafer, D. A. (2005) Ena/VASP proteins enhance actin polymerization in the presence of barbed end capping proteins. *J. Biol. Chem.* **280,** 28653–28662
22. Pasic, L., Kotova, T., and Schafer, D. A. (2008) Ena/VASP proteins capture actin filament barbed ends. *J. Biol. Chem.* **283,** 9814–9819
23. Breitsprecher, D., Kiesewetter, A. K., Linkner, J., Urbanke, C., Resch, G. P., Small, J. V., and Faix, J. (2008) Clustering of VASP actively drives processive, WH2 domain-mediated actin filament elongation. *EMBO J.* **27,** 2943–2954
24. Bear, J. E., Svitkina, T. M., Krause, M., Schafer, D. A., Loureiro, J. J., Strasser, G. A., Maly, I. V., Chaga, O. Y., Cooper, J. A., and Borisy, G. G. (2002) Antagonism between Ena/VASP proteins and actin filament capping regulates fibroblast motility. *Cell* **109,** 509–521
25. Yoshinaga, S., Ohkubo, T., Sasaki, S., Nuriya, M., Ogawa, Y., Yasui, M., Tabata, H., and Nakajima, K. (2012) A phosphatidylinositol lipids system, lamellipodin, and Ena/VASP regulate dynamic morphology of multipolar migrating cells in the developing cerebral cortex. *J. Neurosci.* **32,** 11643–11656
26. Ono, K., Yamashiro, S., and Ono, S. (2008) Essential role of ADF/cofilin for assembly of contractile actin networks in the *C. elegans* somatic gonad. *J. Cell Sci.* **121,** 2662–2670
27. Reymann, A. C., Suarez, C., Guérin, C., Martiel, J. L., Staiger, C. J., Blanchoin, L., and Boujemaa-Paterski, R. (2011) Turnover of branched actin filament networks by stochastic fragmentation with ADF/cofilin. *Mol. Biol. Cell* **22,** 2541–2550
28. Lai, F. P., Szczodrak, M., Block, J., Faix, J., Breitsprecher, D., Mannherz, H. G., Stradal, T. E., Dunn, G. A., Small, J. V., and Rottner, K. (2008) Arp2/3 complex interactions and actin network turnover in lamellipodia. *EMBO J.* **27,** 982–992
29. Kwiatkowski, A. V., Rubinson, D. A., Dent, E. W., Edward van Veen, J., Leslie, J. D., Zhang, J., Mebane, L. M., Philippar, U., Pinheiro, E. M., and Burds, A. A. (2007) Ena/VASP is required for neuritogenesis in the developing cortex. *Neuron* **56,** 441–455
30. Lebrand, C., Dent, E. W., Strasser, G. A., Lanier, L. M., Krause, M., Svitkina, T. M., Borisy, G. G., and Gertler, F. B. (2004) Critical role of Ena/VASP proteins for filopodia formation in neurons and in function downstream of netrin-1. *Neuron* **42,** 37–49
31. Lin, W. H., Nebhan, C. A., Anderson, B. R., and Webb, D. J. (2010) Vasodilator-stimulated phosphoprotein (VASP) induces actin assembly in dendritic spines to promote their development and potentiate synaptic strength. *J. Biol. Chem.* **285,** 36010–36020
32. Fleming, T., Chien, S. C., Vanderzalm, P. J., Dell, M., Gavin, M. K., Forrester, W. C., and Garriga, G. (2010) The role of *C. elegans* Ena/VASP homolog UNC-34 in neuronal polarity and motility. *Dev. Biol.* **344,** 94–106
33. Sarmiere, P. D., and Bamburg, J. R. (2004) Regulation of the neuronal actin cytoskeleton by ADF/cofilin. *J. Neurobiol.* **58,** 103–117
34. Kuhn, T. B., Meberg, P. J., Brown, M. D., Bernstein, B. W., Minamide, L. S., Jensen, J. R., Okada, K., Soda, E. A., and Bamburg, J. R. (2000) Regulating actin dynamics in neuronal growth cones by ADF/cofilin and rho family GTPases. *J. Neurobiol.* **44,** 126–144
35. Tahirovic, S., and Bradke, F. (2009) Neuronal polarity. *Cold Spring Harbor Perspect. Biol.* **1,** 1–17
36. Garvalov, B. K., Flynn, K. C., Neukirchen, D., Meyn, L., Teusch, N., Wu, X., Brakebusch, C., Bamburg, J. R., and Bradke, F. (2007) Cdc42 regulates cofilin during the establishment of neuronal polarity. *J. Neurosci.* **27,** 13117–13129
37. Spudich, J. A., and Watt, S. (1971) The regulation of rabbit skeletal muscle contraction. *J. Biol. Chem.* **246,** 4866–4871
38. Ono, S., Yamakita, Y., Yamashiro, S., Matsudaira, P. T., Gnarra, J. R., Obinata, T., and Matsumura, F. (1997) Identification of an actin binding region and a protein kinase C phosphorylation site on human fascin. *J. Biol. Chem.* **272,** 2527–2533
39. Danino, D., Bernheim-Groswasser, A., and Talmon, Y. (2001) Digital cryogenic transmission electron microscopy: an advanced tool for direct imaging of complex fluids. *Colloids Surf. Physicochem. Eng. Aspects* **183,** 113–122
40. Bernheim-Groswasser, A., Wiesner, S., Golsteyn, R. M., Carlier, M. F., and Sykes, C. (2002) The dynamics of actin-based motility depend on surface parameters. *Nature* **417,** 308–311
41. Siton, O., Ideses, Y., Albeck, S., Unger, T., Bershadsky, A. D., Gov, N. S., and Bernheim-Groswasser, A. (2011) Cortactin releases the brakes in actin-based motility by enhancing WASP-VCA detachment from Arp2/3 branches. *Curr. Biol.* **21,** 2092–2097
42. Kuhn, J. R., and Pollard, T. D. (2005) Real-time measurements of actin filament polymerization by total internal reflection fluorescence microscopy. *Biophys. J.* **88,** 1387–1402
43. Michelot, A., Berro, J., Guérin, C., Boujemaa-Paterski, R., Staiger, C. J., Martiel, J. L., and Blanchoin, L. (2007) Actin-filament stochastic dynamics mediated by ADF/cofilin. *Curr. Biol.* **17,** 825–833
44. Schirenbeck, A., Arasada, R., Bretschneider, T., Stradal, T. E., Schleicher, M., and Faix, J. (2006) The bundling activity of vasodilator-stimulated phosphoprotein is required for filopodium formation. *Proc. Natl. Acad. Sci. U.S.A.* **103,** 7694–7699
45. Neidt, E. M., Scott, B. J., and Kovar, D. R. (2009) Formin differentially utilizes profilin isoforms to rapidly assemble actin filaments. *J. Biol. Chem.* **284,** 673–684
46. Carlier, M. F., Hertzog, M., Didry, D., Renault, L., Cantrelle, F. X., van Heijenoort, C., Knossow, M., and Guittet, E. (2007) Structure, function, and evolution of the β-thymosin/WH2 (WASP-homology2) actin-binding module. *Ann. N.Y. Acad. Sci.* **1112,** 67–75
47. Irobi, E., Aguda, A. H., Larsson, M., Guerin, C., Yin, H. L., Burtnick, L. D., Blanchoin, L., and Robinson, R. C. (2004) Structural basis of actin sequestration by thymosin-β4: implications for WH2 proteins. *EMBO J.* **23,** 3599–3608
48. Andrianantoandro, E., and Pollard, T. D. (2006) Mechanism of actin filament turnover by severing and nucleation at different concentrations of ADF/cofilin. *Mol. Cell* **24,** 13–23
49. Gov, N. S., and Bernheim-Groswasser, A. (2012) Releasing the brakes while hanging on: cortactin effects on actin-driven motility. *Bioarchitecture.* **2,** 11–14
50. Hüttelmaier, S., Harbeck, B., Steffens, O., Messerschmidt, T., Illenberger, S., and Jockusch, B. M. (1999) Characterization of the actin binding properties of the vasodilator-stimulated phosphoprotein VASP. *FEBS Lett.* **451,** 68–74
51. Amann, K. J., and Pollard, T. D. (2001) Direct real-time observation of actin filament branching mediated by Arp2/3 complex using total internal reflection fluorescence microscopy. *Proc. Natl. Acad. Sci. U.S.A.* **98,** 15009–15013
52. Schafer, D. A., Jennings, P. B., and Cooper, J. A. (1996) Dynamics of capping protein and actin assembly *in vitro*: uncapping barbed ends by polyphosphoinositides. *J. Cell Biol.* **135,** 169–179
53. Pollard, T. D., Blanchoin, L., and Mullins, R. D. (2000) Molecular mechanisms controlling actin filament dynamics in nonmuscle cells. *Annu. Rev. Biophys. Biomol. Struct.* **29,** 545–576
54. Ideses, Y., Brill-Karniely, Y., Haviv, L., Ben-Shaul, A., and Bernheim-Groswasser, A. (2008) Arp2/3 branched actin network mediates filopodia-like bundles formation *in vitro*. *PloS One* **3,** e3297
55. Brill-Karniely, Y., Ideses, Y., Bernheim-Groswasser, A., and Ben-Shaul, A. (2009) From branched networks of actin filaments to bundles. *ChemPhysChem* **10,** 2818–2827
56. Haviv, L., Brill-Karniely, Y., Mahaffy, R., Backouche, F., Ben-Shaul, A., Pollard, T. D., and Bernheim-Groswasser, A. (2006) Reconstitution of the transition from lamellipodium to filopodium in a membrane-free system. *Proc. Natl. Acad. Sci. U.S.A.* **103,** 4906–4911
57. Ghosh, M., Song, X., Mouneimne, G., Sidani, M., Lawrence, D. S., and Condeelis, J. S. (2004) Cofilin promotes actin polymerization and defines the direction of cell motility. *Science* **304,** 743–746
58. Achard, V., Martiel, J. L., Michelot, A., Guérin, C., Reymann, A. C., Blanchoin, L., and Boujemaa-Paterski, R. (2010) A "primer"-based mechanism

underlies branched actin filament network formation and motility. *Curr. Biol.* **20,** 423–428
59. Ichetovkin, I., Grant, W., and Condeelis, J. (2002) Cofilin produces newly polymerized actin filaments that are preferred for dendritic nucleation by the Arp2/3 complex. *Curr. Biol.* **12,** 79–84
60. Krause, M., Dent, E. W., Bear, J. E., Loureiro, J. J., and Gertler, F. B. (2003) Ena/VASP proteins: regulators of the actin cytoskeleton and cell migration. *Annu. Rev. Cell Dev. Biol.* **19,** 541–564
61. Bohil, A. B., Robertson, B. W., and Cheney, R. E. (2006) Myosin-X is a molecular motor that functions in filopodia formation. *Proc. Natl. Acad. Sci. U.S.A.* **103,** 12411–12416
62. Applewhite, D. A., Barzik, M., Kojima, S., Svitkina, T. M., Gertler, F. B., and Borisy, G. G. (2007) Ena/VASP proteins have an anti-capping independent function in filopodia formation. *Mol. Biol. Cell* **18,** 2579–2591